

Measurement of Magnetic Susceptibility of Diamagnetic Liquids Exploiting the Moses Effect

D. Shulman,^{1,2} M. Lewkowicz,² and E. Bormashenko¹

¹*Department of Chemical Engineering, Ariel University, Ariel 40700, Israel*

²*Physics Department, Ariel University, Ariel 40700, Israel*

(Dated: June 10, 2022)

A novel comparative technique enabling measurement of the magnetic susceptibility of diamagnetic liquids with the “Moses effect” is presented. The technique is based on the experimental establishment of the deformation of the liquid/vapor interface by a steady magnetic field. The deformation of the liquid surface by a modest magnetic field ($B \sim 0.60T$) is measured with an optical technique. The surface tension of the liquid is taken into account. The magnetic susceptibilities of the investigated liquids (Ethanol and Glycerol) were calculated from the maximal slope of the liquid/air interface. The suggested approach yields an accuracy on the order of about 0.4 – 0.6% and hence is superior to previous methods which used the “Moses effect” for the same purpose.

PACS numbers:

INTRODUCTION

Measurement of magnetic susceptibility of liquids in a non-trivial experimental task [1–7]. The standard methods used to measure the magnetic susceptibility of feebly magnetic objects are based on the measurement of the force acting on the object when placed in a non-uniform magnetic field. In all these methods it is essential that the body can be displaced. The force acting on the body is small, usually only a few dynes, and delicate methods have to be used for achieving accurate measurements, as in the common Curie-Faraday method where the studied object is placed on a sensitive torsion balance [2], [5]. Several methods were used for the measurement of the magnetic susceptibility such as Faraday’s scale, Guoy’s scale or inductive method exploiting the SQUID magnetometer [2]. A nuclear magnetic resonance (NMR) method was effectively used for measuring the magnetic susceptibility of bar-shaped samples that have an arbitrary cross-section and do not produce the MR signal [4], [6]. Magnetic susceptibility of a broad variety of materials was studied systematically with a magnetic resonance recently in ref. [7].

Measurement of magnetic susceptibility of liquids poses additional experimental problems. These problems were surmounted by Broersma, who applied the torsion balance and an inductance apparatus for the precise measurement of magnetic susceptibility of diamagnetic organic liquids [1]. In parallel, magnetic susceptibility of diamagnetic organic liquids was studied with NMR in ref. [7]. Recently the method of the measurement of diamagnetic liquids based on the Moses effect was introduced [3]. Moses effect is a phenomenon of deformation of the surface of a diamagnetic liquid by a magnetic field [8–14].

Moses effect is a relatively weak phenomenon: the application of magnetic fields on the order of magnitude of 0.1 – 1T results in the formation of a near-surface “well”

with a depth of dozens of micrometers [10]. However, it is sufficient for the measurement of the magnetic susceptibility of the studied diamagnetic liquids, as shown in ref. [3], in which the deformation of the liquid surface by a magnetic field was determined by a laser bounce. The analysis of the shape of the near-surface “well” produced by the magnetic field yielded the value of the magnetic susceptibility. We demonstrate, how the accuracy of the Moses Effect method, introduced in ref. [3], may be essentially improved, under considering interfacial effects, namely the energy of the deformed liquid/vapor interface.

THEORETICAL BASIS OF THE SUGGESTED EXPERIMENTAL METHOD

The original theory of the Moses effect [11] implies that the shape of the “dip” formed by the permanent magnet emerges as a minimum of the sum of the gravitational and magnetic energies. Assuming a cylindrically symmetrical magnetic field $\vec{B}(r, h)$ the following expression is predicted [3, 10, 15] for the shape of the well $z(r)$, schematically shown in Fig. (1):

$$z(r, h) = \frac{\chi B^2(r, h)}{2\mu_0 \rho g}. \quad (1)$$

χ and ρ are the magnetic susceptibility and the density of the liquid, respectively, and h is the separation between the magnet and non-deformed liquid/vapor interface.

Eq.(1) neglects the surface tension of the liquid/vapor interface. Thus, the magnetic susceptibility according to Eq.(1) inevitably includes a systematic error. We introduce a model that includes the surface tension, so that a more accurate prediction of the magnetic susceptibility of diamagnetic liquids becomes possible.

The Young-Laplace equation defining the shape of the liquid-air interface deformed by a time-independent magnetic field, which takes into account surface tension γ is derived in [10]:

$$\frac{\partial^2 z}{\partial r^2} + \frac{1}{r} \frac{\partial z}{\partial r} - \frac{\rho g}{\gamma} z = \frac{\chi B^2(r, h)}{2\mu_0 \gamma} \quad (2)$$

with its solution

$$z(r, h) = - \left[\int_0^r \frac{\chi B^2(r, h)}{2\mu_0 \gamma} I_0(\lambda_c^{-1} r) r dr \right] K_0(\lambda_c^{-1} r) - \left[\int_r^\infty \frac{\chi B^2(r, h)}{2\mu_0 \gamma} K_0(\lambda_c^{-1} r) r dr \right] I_0(\lambda_c^{-1} r). \quad (3)$$

Here $I_\alpha(x)$ and $K_\alpha(x)$ are the modified Bessel functions of the first and the second kind, respectively.

The interplay between the gravity and the surface tension is quantified by the capillary length, denoted λ_c (see [17–19]), defined as:

$$\lambda_c = \sqrt{\frac{\gamma}{\rho g}}. \quad (4)$$

It is noteworthy that the value of the capillary length is of the order of a few millimeters for a majority of liquids, in particular for water $\lambda_{c, H_2O} = 2.71 \text{ mm}$ (see [10],[16–18]). The physical properties of the liquids used in our investigation are supplied in Table 1. The values of the capillary lengths calculated for the studied liquids are confined in the range of $\lambda_c \cong 1.7 - 7.2 \text{ mm}$ (see Table 1). The typical scale at which the shape of the near-surface well is constituted is on the order of magnitude of $\sim 10 \text{ mm}$, as recognized from Figure 2; thus the effects due to the surface tension are well expected to be

essential. Measuring the surface well profile $z(r, h)$ and obtaining the magnetic susceptibility from Eq.(1) (which neglects the surface tension), as reported in [3], inevitably generates a relatively high error of χ .

We suggest an experimental procedure that enables a more accurate estimate of the magnetic susceptibility of diamagnetic liquids, due to two essential improvements, namely:

- 1) Considering the effects of the surface tension and the use of the solution of the Young-Laplace equation which yields a more faithful shape of the liquid surface deformed by the magnetic field;
- 2) Use of the maximal slope of the near-surface well for the calculation of the magnetic susceptibility of the addressed diamagnetic liquids.

The measurement of the maximal slope angle θ_m of the liquid/vapor interface enables an accurate establishment of the magnetic susceptibility. For small curvature $dz/dr \ll 1$, so that $dz/dr \cong \theta$, see Fig. 1. The derivative of Eq.(3):

$$\theta = \frac{dz}{dr} = \left[\int_0^r \frac{\chi B^2(r, h)}{2\mu_0 \gamma} I_0(\lambda_c^{-1} r) r dr \right] \lambda_c^{-1} K_1(\lambda_c^{-1} r) - \left[\int_r^\infty \frac{\chi B^2(r, h)}{2\mu_0 \gamma} K_0(\lambda_c^{-1} r) r dr \right] \lambda_c^{-1} I_1(\lambda_c^{-1} r) \quad (5)$$

Denoting the distance from the axis of the magnet to the point of maximal slope as r_m , and inverting Eq.(5), yields an expression for the magnetic susceptibility:

$$\chi = \theta_m \cdot \left\{ \left[\int_0^{r_m} \frac{B^2(r, h)}{2\mu_0 \gamma} I_0(\lambda_c^{-1} r) r dr \right] \lambda_c^{-1} K_1(\lambda_c^{-1} r_m) - \left[\int_{r_m}^\infty \frac{B^2(r, h)}{2\mu_0 \gamma} K_0(\lambda_c^{-1} r) r dr \right] \lambda_c^{-1} I_1(\lambda_c^{-1} r_m) \right\}^{-1} \quad (6)$$

Assuming that the space dependence of the magnetic field $\vec{B}(r, h)$ is known, one could find r_m from the second derivative of $z(r, h)$ which vanishes at θ_m :

$$\begin{aligned} \frac{d^2 z}{dr^2} &= \frac{\chi B^2(r, h)}{2\mu_0 \gamma} - \left[\int_0^r \frac{\chi B^2(r, h)}{2\mu_0 \gamma} I_0(\lambda_c^{-1} r) r dr \right] \lambda_c^{-2} \left(K_0(\lambda_c^{-1} r) + \frac{1}{\lambda_c^{-1} r} K_1(\lambda_c^{-1} r) \right) \\ &\quad - \left[\int_r^\infty \frac{\chi B^2(r, h)}{2\mu_0 \gamma} K_0(\lambda_c^{-1} r) r dr \right] \lambda_c^{-2} \left(I_0(\lambda_c^{-1} r) - \frac{1}{\lambda_c^{-1} r} I_1(\lambda_c^{-1} r) \right) \end{aligned} \quad (7)$$

and hence

$$B^2(r_m, h) = \left[\int_0^{r_m} B^2(r, h) I_0(\lambda_c^{-1}r) r dr \right] \lambda_c^{-2} \left(K_0(\lambda_c^{-1}r_m) + \frac{1}{\lambda_c^{-1}r_m} K_1(\lambda_c^{-1}r_m) \right) - \left[\int_{r_m}^{\infty} B^2(r, h) K_0(\lambda_c^{-1}r) r dr \right] \lambda_c^{-2} \left(I_0(\lambda_c^{-1}r_m) - \frac{1}{\lambda_c^{-1}r_m} I_1(\lambda_c^{-1}r_m) \right) \quad (8)$$

The only unknown variable r_m in Eq.(8) can be found by numerical methods [19] if the space dependence of the magnetic field $\vec{B}(r, h)$ is known. Albeit, an accurate measurement of this space dependence of the magnetic field is challenging and poses essential experimental problems. The inaccuracy in the measurement of the magnetic field introduces the main experimental error in the assessment of the magnetic susceptibility of diamagnetic liquids. We can avoid this problem using the following experimental comparative procedure: water (a diamagnetic liquid with a well-known magnetic susceptibility $\chi_{H_2O} = -9.035 \cdot 10^{-6}$ [24]) is used as “calibration liquid”. The shape of the well produced in water by the magnet and the value of r_m can be established as described in detail in the Experimental Section. Thus, the space dependence of the magnetic field can be extracted from the shape of the near-surface well produced in the “calibration liquid” (water) as described in detail in Appendix A. This magnetic field $\vec{B}(r, h)$ will be used for the measurement of the magnetic susceptibility of other diamagnetic liquids, as glycerol and ethanol in this study. The value of the magnetic susceptibility is then calculated from Eq.(6).

MATERIALS AND METHOD

The suggested experimental technique for the measurement of the magnetic susceptibility of diamagnetic liquids is based on the profile of the near-surface well forced in the liquid by a permanent magnetic field. The main elements of the experimental unit, shown in Figs.(3) and (4) are:

- 1) the sample liquid placed into a Petri dish $\varnothing 90mm$
- 2) a 633nm He-Ne laser (4mW 1107/P JDS Uniphase Corporation)
- 3) a stack of neodymium permanent magnets (Magsy)
- 4) XYZ gantry, in-house assembled from CCM Automation Technology components
- 5) digital camera, (8.0 megapixel digital bridge camera Sony Cyber-shot DSC-F828)
- 6) GM2 Gauss meter (AlphaLab Inc, USA), accuracy 1%

The Petri dish with the liquid sample filled to a depth of $1 \pm 0.2cm$ was set on top of a frame constructed from non-ferromagnetic material (see Figs.(3) and (4)). A cylindrical bar magnet of neodymium (*NdFeB*) with the diameter 22.8mm and length 30mm was used. The magnetic field strength at the base center was $B_z = 0.60 \pm 0.01T$.

The magnetic field was modelled as an ideal solenoid [20–23]. The measured magnetic field showed good similarity with the solenoid field. Fig.(7) shows a comparison of both fields at a distance of $h = 0.5mm$ from the magnet’s base. The location of the magnet was fixed with the XYZ actuator with an accuracy of $10\mu m$. In the experiments an Arduino controller for the step motors was used. Fig.(3) shows the experimental set-up to measure the exact separation of the magnet from the liquid surface h . The minimum step of the XYZ actuator was $10\mu m$.

The position of the laser beam on the screen was registered with the digital camera. The experiments were carried out under ambient conditions ($P = 1atm; T = 25 \pm 1^{\circ}C$). A photograph of the experimental unit is shown in Fig.(4).

The investigated liquids, see Table 1, were exposed to the permanent magnetic field; the surface of the liquid was illuminated with the laser beam as shown in Fig. (5).

The deformation profile of the liquid sample is measured with the Ne-He laser. Its beam diameter is 0.48mm and the beam divergence 1.7mrad. The angle of incidence Θ on the surface of the liquid is about 5° . The inclination of the curved surface was extracted from the angle of reflection of the laser beam.

When the fluid is deformed by a magnetic field by an angle $\Delta\theta$, the reflection angle shifts by $2\Delta\theta$, which causes a corresponding shift in height Δz on the screen, as shown in Fig.(5). Hence we have the following relationship for the change in the angle of reflection:

$$2\Delta\theta = \arctan\left(\frac{y + \Delta y}{r}\right) - \Theta \quad (9)$$

The laser spot was captured on the screen with the digital camera while displacing the magnet horizontally. Further video processing enabled the determination of the maximal surface slope θ_m which in turn yields r_m in

Eq.(8). Substituting θ_m and r_m into Eq.(6) allows the calculation of the magnetic susceptibility of the studied liquid χ .

The measurement was performed as follows: the magnet was fixed at the XYZ precision stage, which displaced the magnet, as shown in Figs.(5) and (6). The laser beam scanned the curved liquid/vapor interface. The XYZ stage lifted the magnet vertically with the step of $0.1mm$ and the scanning was repeated. The maximal slope of the liquid/air interface was established at each

height. An arithmetic mean of the magnetic susceptibility was accepted as a statistically reliable value.

The materials used in the experiments:

1. Distilled water, prepared by using a Synergy ultraviolet water purification system (Millipore Sas, France)
2. Ethanol (Bio-Lab Ltd., Israel)
3. Glycerol (J.T. Baker Chemicals, Holland)
4. Calcium chloride (Merck KGaA, Germany)
5. Sodium chloride (Sigma-Aldrich, Germany)

Table 1

Liquid	Density ρ [$\frac{g}{cm^3}$]	Surface Tension γ [$\frac{mJ}{m^2}$]	Capillary length λ_c [mm]
Water	0.998	72.8	2.71
Glycerol	0.126	64.0	7.20
Ethanol	0.789	22.1	1.69

The liquids' parameters, at room temperature.

RESULTS AND DISCUSSION

The suggested method does not measure the magnetic field directly, which inevitable would give rise to relatively large errors, resulting in large errors in the measurement of magnetic susceptibility. Rather, a comparative method of measurement was exploited: the measurement was calibrated with water at standard conditions, which has a well-known magnetic susceptibility χ .

The experimentally established values of the volume magnetic susceptibility (in SI units) for Ethanol and Glycerol were $\chi_{ethanol} = -7.23 \cdot 10^{-6} \pm 0.03 \cdot 10^{-6}$ and $\chi_{glycerol} = -9.83 \cdot 10^{-6} \pm 0.06 \cdot 10^{-6}$, correspondingly. The deviation of the reported results from the literature data [24] was 0.6% for ethanol and 0.39% for glycerol. The comparison of the experimentally obtained and literature data is shown in Fig.(6).

For the measurement of the magnetic susceptibility of salt solutions we choose $NaCl$ and $CaCl_2$. The experimental values for these compounds are summarized in Table 2. Calculation of the susceptibilities of dissolved salts has usually been based on the assumptions that the susceptibility of the solution varies linearly with concentration and that the susceptibility of the solvent is not affected by the presence of dissolved salts [25]. The validity of these assumptions can be verified by the experimental data, see Fig.(6). The assumption of a linear dependence of the susceptibility of solutions with concentration seems to be justified for many simple salts by the results obtained. In most cases the susceptibility of the salt in the dissolved state is greater than it in the crystalline state [25].

Table 2. Volume susceptibility (in SI units)

	crystalline state ⁽¹⁾	aqueous solution ⁽¹⁾	aqueous solution ⁽²⁾
	$\chi_{crystal}$	$\chi_{dissolved}^{(1)}$	$\chi_{dissolved}^{(2)}$
$NaCl$	$-1.40 \cdot 10^{-5}$	$-1.41 \cdot 10^{-5}$	$-1.40 \cdot 10^{-5}$
$CaCl_2$	$-1.33 \cdot 10^{-5}$	$-1.36 \cdot 10^{-5}$	$-1.37 \cdot 10^{-5}$

(1) from ref. [25]

(2) our experimental value

In order to demonstrate the improved accuracy of the suggested experimental technique the effect of the surface tension was analyzed in Appendix B. The effect is substantial for radii of the magnet smaller than the capillary length, Eq.(4), for larger radii it becomes negligible, though. Albeit, the use of "giant magnets" would render the method cumbersome.

CONCLUSION

The "Moses Effect" enables an accurate experimental measurement of the magnetic susceptibility of diamagnetic liquids when interfacial phenomena effects are considered. Magnetic susceptibility of diamagnetic liquids was already calculated from the shape of the well created by a magnetic field in the studied liquid [3]. The method reported in ref. [3] neglects the effect of the surface tension. We improve the method suggested in ref. [3] as follows: i) the effects due to the surface tension are considered; ii) a comparative method is suggested using water a calibration liquid; iii) the magnetic susceptibility of the investigated liquids are found from the maximal slope of the liquid/air interface.

APPENDIX A.

In order to determine the magnetic susceptibility with (6) one needs the explicit spatial distribution of the mag-

netic field produced by the permanent magnet, $\vec{B}(r, h)$. This distribution was approximated by the ideal solenoid model described by the following equations [20]

$$B_r(r, h) = B_0 \int_0^{\pi/2} d\psi (\cos^2 \psi - \sin^2 \psi) \left\{ \frac{\alpha_+}{\sqrt{\cos^2 \psi + k_+^2 \sin^2 \psi}} - \frac{\alpha_-}{\sqrt{\cos^2 \psi + k_-^2 \sin^2 \psi}} \right\}$$

$$B_z(r, h) = \frac{B_0 a}{r + a} \int_0^{\pi/2} d\psi \left(\frac{\cos^2 \psi + \tau \sin^2 \psi}{\cos^2 \psi + \tau^2 \sin^2 \psi} \right) \left\{ \frac{\beta_+}{\sqrt{\cos^2 \psi + k_+^2 \sin^2 \psi}} - \frac{\beta_-}{\sqrt{\cos^2 \psi + k_-^2 \sin^2 \psi}} \right\}$$

$$\alpha_{\pm} = \frac{a}{\sqrt{h_{\pm}^2 + (r + a)^2}}, \quad \beta_{\pm} = \frac{h_{\pm}}{\sqrt{h_{\pm}^2 + (r + a)^2}}$$

$$h_+ = h, \quad h_- = h - 2b, \quad \tau = \frac{a - r}{a + r}$$

$$k_{\pm} = \sqrt{\frac{h_{\pm}^2 + (a - r)^2}{h_{\pm}^2 + (a + r)^2}}$$

where a is the radius and $2b$ is the length of the solenoid, equal to the radius and the length of our permanent magnet, and B_0 is a constant with units *tesla*. In order to calculate the magnetic susceptibility χ , Eq.(6), one needs to know the value of B_0 , albeit an accurate measurement of B_0 is accompanied with considerable experimental challenges.

To determine the numerical value of B_0 we use water as a calibration liquid, its physical properties (namely: density ρ , surface tension γ and magnetic susceptibility χ) being well-known [24]. Measuring the maximal slope θ_m for water and inverting Eq.(5) results in the value $B_0 = 1.2T$. To improve the accuracy of the measurement the experiments were repeated at different separations h . The comparison of the experimentally established radial dependence of the magnetic field with that calculated with the above equations is depicted in Fig.(7).

APPENDIX B:

Influence of the surface tension on the accuracy of the measurement Various groups determined the

magnetic susceptibility of diamagnetic liquids with the Moses effect [3], where the magnetic susceptibility was derived from the well's profile created by the magnetic field. The calculation based on the Eq. (1) neglects the effect of the liquid's surface tension. Here we estimate the error arising from ignoring the interfacial effects, i.e., we compare the values of the magnetic susceptibilities derived from Eq. (1) and Eq. (6).

To compare the two methods, we introduce a dimensionless number $\eta = \chi_1/\chi_2$, the ratio between the values of the magnetic susceptibility obtained under considering surface tension, denoted χ_1 , and neglecting surface tension, denoted χ_2 .

An interplay between the effects due to gravity and surface tension is quantified by the capillary length $\lambda_c = \sqrt{\frac{\gamma}{\rho g}}$ introduced in Section 2. Let us define the dimensionless number ξ relating the radius of the magnet for the deformation of the liquid/vapor interface to the capillary length defined as follows: $\xi = (R_{magnet}/\lambda_c)^2$. In Fig. (8) the dependence of the accuracy of our measurement η on the parameter ξ is shown. As ξ increases, the effect of the surface tension decreases, and the interfacial effects become negligible.

Indeed, the interplay between the effects due to gravity and surface tension for the addressed experimental situation may be quantified by the dimensionless number ζ defined as follows:

$$\zeta = \frac{\gamma 2\pi r}{\rho\pi r^2 Hg} = \frac{\gamma 2}{\rho r Hg}$$

where r and H are the radius and depth of the near-surface well, correspondingly. The radius increases obviously with R_{magnet} . The parameter ζ scales as $1/r$ for the fixed depth of the well. Thus, with the increase of the radius of the magnet the effects due to surface tension disappear.

We conclude that the effects due to the surface tension become negligible when the radii of the magnets are much larger than the capillary length.

-
- [1] S. Broersma. The magnetic susceptibility of organic compounds, *J. Chem. Phys.* **17**, 873 (1949).
- [2] P. Marcon, and K. Ostanina. Overview of methods for magnetic susceptibility measurement. *PIERS Proceedings* (2012).
- [3] Z. Chen, J. Ellis and E. D. Dahlberg. A simple technique to measure the magnetic susceptibility of liquids. *Rev. Sci. Instrum.* **83**, 095112 (2012).
- [4] K. Frei and H.J. Bernstein. Method for determining magnetic susceptibilities by NMR. *J. Chem. Phys.* **37**, 1891 (1962).
- [5] P.L. Kapitza and W.L. Webster. A method of measuring magnetic susceptibilities. *Proc. R. Soc. Lond. A* **132**, 442 (1931).
- [6] P. Marcon, K. Bartusek, M. Burdkova and Z. Dokuopil. Magnetic susceptibility measurement using 2D magnetic resonance imaging. *Meas. Sci. Technol.* **22**, 105702 (2011).
- [7] M. C. Wapler, J. Leupold, I. Dragonu, D. von Elverfeld, M. Zaitsev and U. Wallrabe. Magnetic properties of materials for MR engineering, micro-MR and beyond. *J. Magn. Reson.* **242**, 233, (2014). <https://doi.org/10.1016/j.jmr.2014.02.005> micro-MR and beyond. *J. Magn. Reson.* **242**, 233, (2014). <https://doi.org/10.1016/j.jmr.2014.02.005>
- [8] E. Bormashenko. Moses effect: Physics and applications. *Adv. Colloid Interface Sci.* **269**, 1 (2019).
- [9] Z. Chen and E. D. Dahlberg. Deformation of water by a magnetic field. *Phys. Teach.* **49**, 144 (2011).
- [10] O. Gendelman, M. Frenkel, V. Fliagin, N. Ivanova, V. Danchuk, I. Legchenkova, A. Vilks and E. Bormashenko. Study of the displacement of floating diamagnetic bodies by a magnetic field. *Surf. Innov.* **7**, 194 (2019). <https://doi.org/10.1680/jsuin.18.00064>.
- [11] N. Hirota, T. Homma, H. Sugawara, K. Kitazawa, M. Iwasaka, S. Ueno, H. Yokoi, Y. Kakudate, S. Fujiwara and M. Kawamura. Rise and fall of surface level of water solutions under high magnetic field. *Jpn. J. Appl. Phys.* **34**, L991 (1995). K. Kitazawa, Y. Ikezoe, H. Uetake, N. Hirota. Magnetic field effects on water, air and powders. *Physica B: Condensed Matter* **294–295**, 709 (2001). doi:10.1016/S0921-4526(00)00749-3
- [12] S. Ueno and M. Iwasaka. Properties of diamagnetic fluid in high gradient magnetic fields. *J. Appl. Phys.* **75**, 7177 (1994).
- [13] S. Ueno and M. Iwasaka. Parting of water by magnetic fields. *IEEE Trans. Magn.* **30**, 4698 (1994).
- [14] H. Sugawara, N. Hirota, T. Homma, M. Ohta, K. Kitazawa, H. Yokoi, Y. Kakudate, S. Fujiwara, M. Kawamura, S. Ueno and others. Magnetic field effect on interface profile between immiscible nonmagnetic liquids - Enhanced Moses effect. *J. Appl. Phys.* **79**, 4721 (1996).
- [15] L. D. Landau, J. S. Bell, M. J. Kearsley, L. P. Pitaevskii, E. M. Lifshitz and J. B. Sykes. *Electrodynamics of Continuous Media* (Elsevier Butterworth-Heinemann, Oxford, 1984).
- [16] P.G. de Gennes, F. Brochard-Wyart, D. Quéré. *Capillarity and Wetting Phenomena* (Springer, Berlin, 2003).
- [17] Erbil H.Y. *Surface Chemistry of Solid and Liquid Interfaces* (Wiley-Blackwell, Oxford, 2006).
- [18] E. Bormashenko. *Physics of Wetting: Phenomena and Applications of Fluids on Surfaces* (De Gruyter, Berlin, Boston 2017). <https://doi.org/10.1515/9783110444810>
- [19] P. Virtanen, R. Gommers, T.E. Oliphant, et al. SciPy 1.0: fundamental algorithms for scientific computing in Python. *Nat Methods* **17**, 261 (2020). <https://doi.org/10.1038/s41592-019-0686-2>
- [20] N. Derby and S. Olbert. Cylindrical magnets and ideal solenoids. *Am. J. Phys.* **78**, 229 (2010).
- [21] M. Ortner and L. G. C. Bandeira. Magpylib: A free Python package for magnetic field computation. *SoftwareX* **11**, 100466, (2020). <https://doi.org/10.1016/j.softx.2020.100466>
- [22] J.T. Conway. Exact solutions for the magnetic fields of axisymmetric solenoids and current distributions. *IEEE Trans. Magn.* **37**, 2977 (2001). doi: 10.1109/20.947050
- [23] V. Labinac, N. Erceg and D. Kotnik-Karuzza. Magnetic field of a cylindrical coil. *Am. J. Phys.* **74**, 621 (2006).
- [24] W. M. Haynes. *CRC Handbook of Chemistry and Physics* (CRC Press, 2014).
- [25] F.E. Hoare and G.W. Brindley. The diamagnetic susceptibilities of dissolved and hydrated salts. *Proc. Phys. Soc.* **49**, 619 (1937).

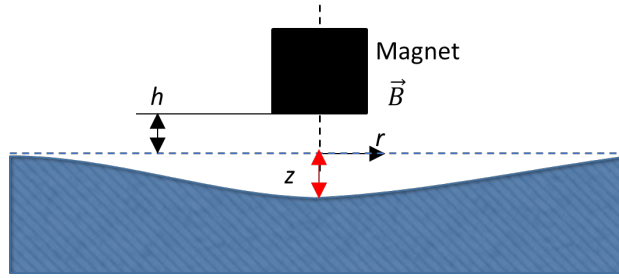


FIG. 1: Shape of the near-surface well arising from the deformation of the liquid/vapor interface by the permanent magnetic field \vec{B} is depicted.

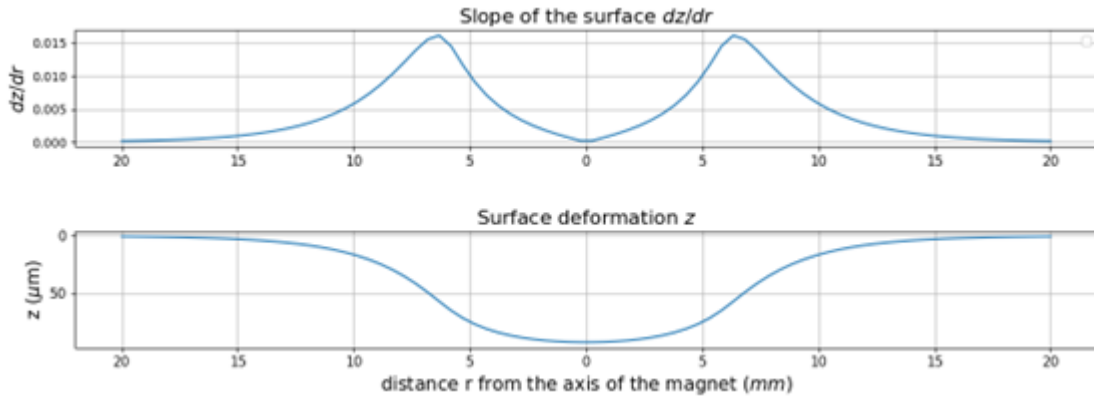


FIG. 2: The water curvature (lower inset) and the slope of the curvature (upper inset) for the magnet with radius $a = 3 \text{ mm}$, placed at the distance of $h = 0.5 \text{ mm}$ from the liquid/vapor interface, as calculated from the Eqs. (3) and (4) respectively are depicted.

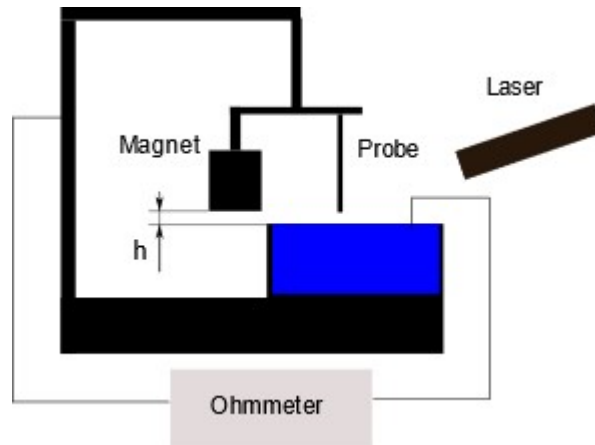


FIG. 3: The scheme of the experimental unit is shown.

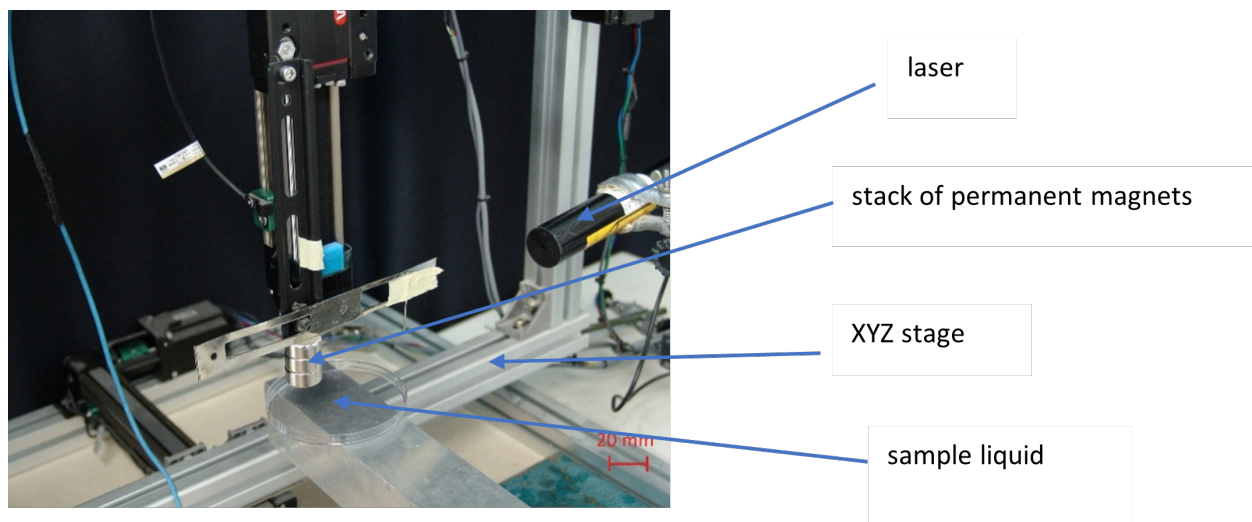


FIG. 4: The set-up of the experimental unit.

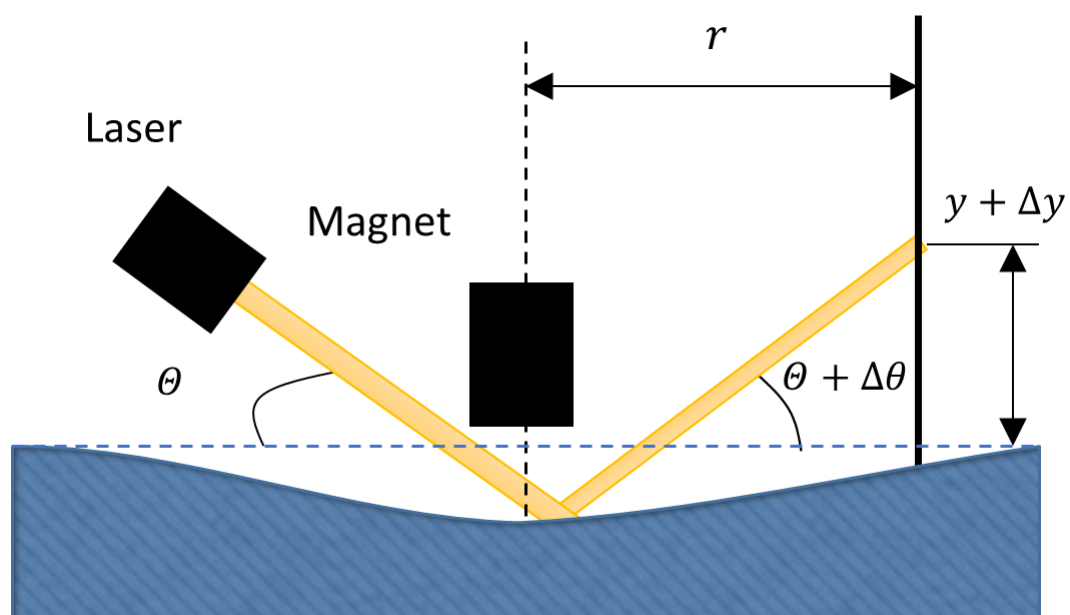
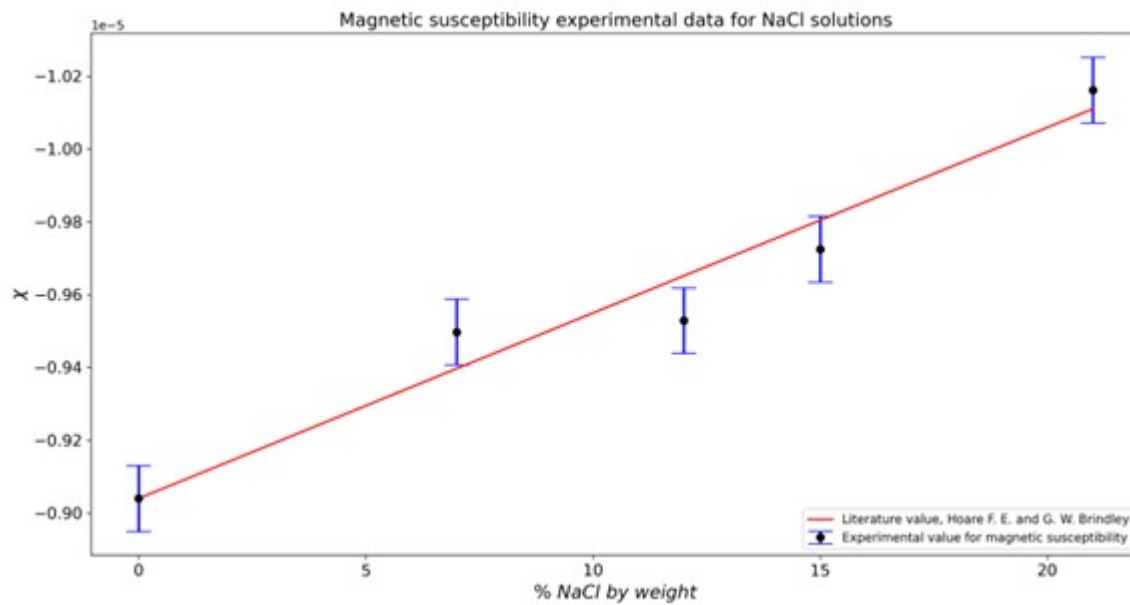


FIG. 5: Scheme of the experimental unit used for the measurement of the magnetic susceptibility of liquids.



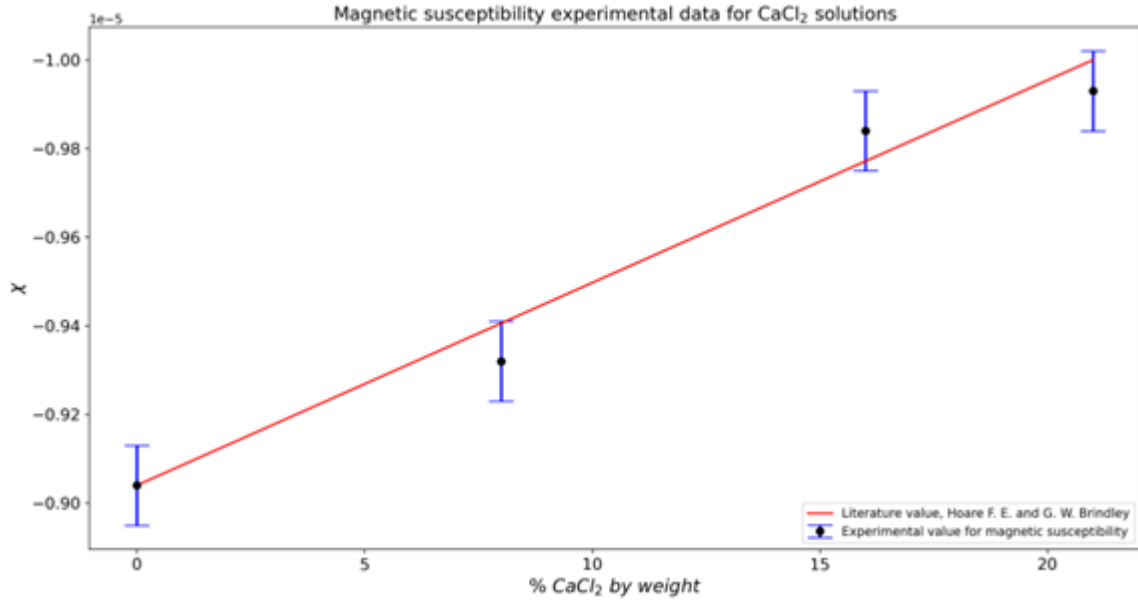


FIG. 6: Values of the magnetic susceptibility extracted from the experimental data (black circles) for various salt solutions in water are depicted. Red solid straight line depicts the literature value of the magnetic susceptibility taken from ref.[24].

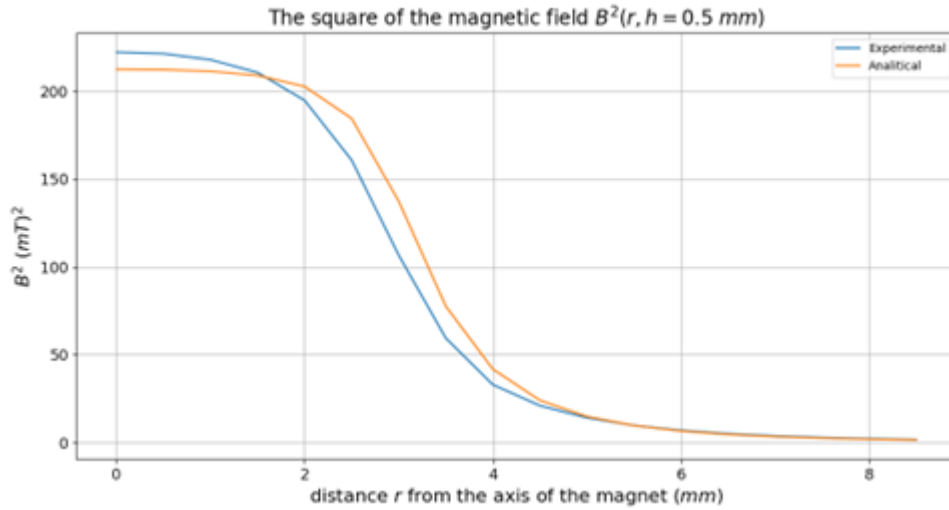


FIG. 7: The comparison of the squared magnetic field $B^2(r) = B_r^2(r) + B_z^2(r)$ as established experimentally (blue curve) and calculated (brown curve) with Eq. A1a-A1b at a distance of $h = 0.5 \text{ mm}$ from the surface of the magnet is shown. The diameter of the magnet is 6 mm.

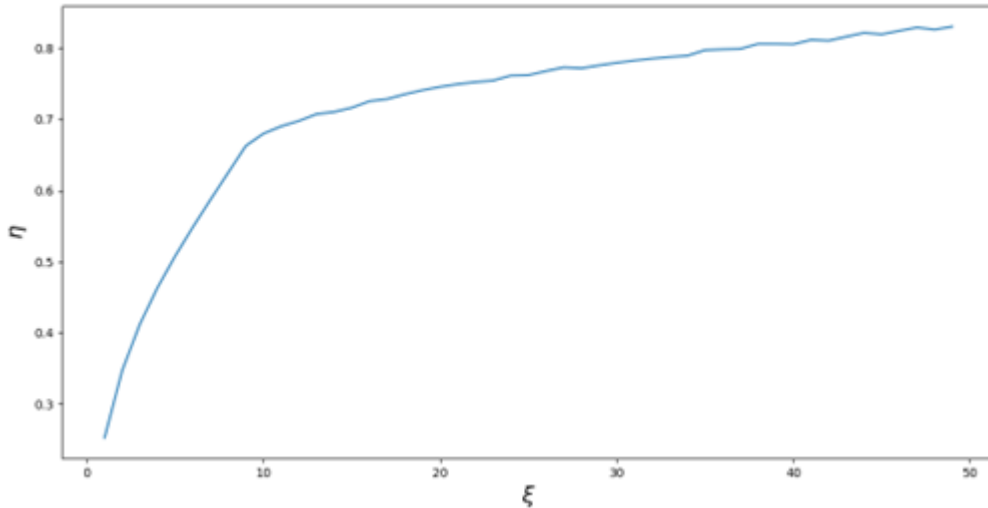


FIG. 8: The dependence of the parameter $\eta = \frac{\chi_1}{\chi_2}$ on the dimensionless number ξ .